

## MECHANICS OF BEDLOAD RATING CURVE SHIFTS AND BEDLOAD HYSTERESIS IN THE TRINITY RIVER, CALIFORNIA

David Gaeuman, Physical Scientist, Trinity River Restoration Program, PO Box 1300  
Weaverville, CA 96093, 530 623-1813; dgaeuman@usbr.gov

**Abstract** Spatial and temporal variability in the entrainment thresholds for various bed surface particle size classes were examined using numerous bedload sediment samples obtained in the Trinity River of Northern California. These data incorporate spatial variability in that bedload samples were obtained at 4 sampling locations spanning 26 kilometers of stream length, and temporal variability in the form of inter-annual shifts in bedload rating curves and clockwise hysteresis over individual flood hydrographs.

Analysis of bedload samples collected on the rising and falling limbs of the 2008 peak flow event suggests that reference shear stresses for the mean surface particle sizes ( $\tau_{rm}$ ) remain relatively constant over time at individual sampling locations. Reference shear stresses for particle size classes similar to the mean surface particle sizes at individual sampling locations remained nearly constant over the course of the flood even where bedload hysteresis was pronounced. Conversely, hiding and exposure effects among different bed surface particles sizes appear to change systematically over the course of the flow release. Reference shear stresses for particle size class  $i$  ( $\tau_{ri}$ ) are typically smaller than  $\tau_{rm}$  when fraction  $i$  is finer than the mean bed surface particle size on both the rising and falling limbs of the hydrograph. However, values of  $\tau_{ri}$  determined for the finer particle fractions on the falling limb of the flood are larger than values determined for the rising limb, with the falling-limb values converging toward  $\tau_{rm}$ . This convergence implies that conditions of equal mobility were more closely approximated on the falling limb of the flood than on the rising limb. Because an increase in  $\tau_{ri}$  for the finer half of the particle distribution implies smaller transport rates for those size classes, the convergence toward equal mobility partially explains the clockwise hysteresis observed in the Trinity bedload samples. Changes in particle entrainment thresholds are also evident in fractional bedload rating curves developed for the rising and falling hydrograph limbs, which frequently indicate that the critical discharge for initiation of transport ( $Q_c$ ) are greater on the falling limb of the flood than on the rising limb. Temporal changes in the abundance of particles available for transport in the finer particle size classes also contribute to bedload hysteresis, particularly for the finer particle size fractions. Values of  $\tau_{ri}$  for size fractions similar to or coarser than the mean bed surface particle size exhibit relatively little temporal variability, and the corresponding rating curves showed relatively little change in  $Q_c$  over the course of the flood event. The mechanisms responsible for hysteresis in the transport rates of these coarser size fractions remain unclear.

### INTRODUCTION

Of the many equations for predicting bedload transport rates in streams that have been proposed over the past 100-plus years, none have proved to be generally reliable (Gomez and Church 1989; Ashmore and Church 1998; McLean et al. 1999; Barry et al. 2004). Although a given equation may produce reasonable predictions of bedload transport rates in a particular stream reach at a particular time, the same equation could be in error by orders of magnitude when applied to a different reach or even to the same reach at a different time. To improve on this

situation, it is necessary to consider how variability in the bedload transport rates in different, but seemingly similar, fluvial settings can be expressed within the conceptual framework of bedload transport theory.

A sediment monitoring program conducted on the gravel-bed Trinity River in Northern California provides an opportunity to investigate spatial and temporal variability in sediment transport rates at multiple locations along the same stream under semi-controlled environmental conditions. The Trinity River is regulated by dams that allow for scheduled bedload sampling during annual high flow releases. Bedload sampling has been conducted annually since 2004 at 4 different transects spanning 26 kilometers of stream length. In many instances, the samples suggest that bedload transport rates undergo a clockwise hysteresis over the course of a single release hydrograph. That is, transport rates on the rising limb of the release are often significantly higher than transport rate at the same discharge on the falling limb. Although this type of hysteresis is common when considering the suspended transport of fine sediments, it is not often described in the context of bed-material transport in gravel-bed streams. Moreover, gravel transport formulae generally lacks a means to explicitly account for bedload hysteresis – only indirect effects, such as a change in the bed surface particle size distribution over the course of the hydrograph, can be accommodated.

This paper investigates the mechanisms of bedload hysteresis in the Trinity River within the conceptual structure provided by surface-based bedload transport equations of the type advanced by Parker (1990) and Wilcock and Crowe (2003). Equations of this type consist of 3 basic components: a means to specify a reference shear stress that produces a small but measurable transport rate for the mean particle size on the stream bed [ $\tau_{rm}$ ], a hiding-exposure function for extrapolating  $\tau_{rm}$  to determine similar reference shears stresses for other particle size fractions present on the stream bed [ $\tau_{ri}$ , where  $i$  denotes particle size class  $i$ ], and a non-dimensional transport function [ $W^* = f(\tau/\tau_{ri})$ ].

There are essentially 4 ways bedload hysteresis can be accommodated in this structure. The most straight-forward way is simply that the finer particle size classes may be winnowed from the bed surface during the flow event so that fewer of the most mobile particles are available for transport on the falling limb. This possibility is inherently incorporated in the transport formulae, because by definition  $W^*$  is scaled by  $F_i$ , the fraction of particle size class  $i$  ( $D_i$ ) present on the bed surface. Another possibility is that changes in the bed surface texture increase the value of  $\tau_{rm}$  irrespective of any actual changes in the mean particle size on the bed surface ( $D_m$ ). In other words, the dimensionless reference shear stress for  $D_m$  ( $\tau_{*rm}$ ) increases. A third potential mechanism that could lead to bedload hysteresis is that changes in the bed surface texture modify the hiding-exposure function so that the relative magnitudes of  $\tau_{ri}$  and  $\tau_{rm}$  are altered. A final possibility it that changes in the bed surface texture modify  $W^*$ .

The investigation reported herein is focused primarily on the third possibility: whether changes in the hiding-exposure function might account for bedload hysteresis. This addresses the general question of whether it is possible to specify a single hiding-exposure relation that is applicable to a wide range of transport conditions, or whether hiding-exposure effects are sensitive to minor differences in the bed surface state. The form of the hiding-exposure functions used with the type of bedload equations considered here is:

$$\tau_{ri}/\tau_{rm} = (D_i/D_m)^h \quad (1)$$

The value of the exponent  $h$  quantifies the degree to which the mobility of sediment particles is determined by their size, as opposed to their relative exposure to the flow. An exponent of 1 would mean that the ratio of reference shear stresses for particles of different sizes is exactly proportion to the ratio of their sizes, and corresponds to perfect size-selective transport. An exponent of zero would indicate that  $\tau_r$  is identical for all particle sizes, and correspond to perfect equal mobility. Values reported for this exponent range from near zero to about 0.3, although values in the vicinity of 0.1 are perhaps most common (Parker and Klingeman 1982; Ashworth and Ferguson 1989; Ferguson et al. 1989; Parker 1990; Andrews 1994).

## DATA AND METHODS

Bedload samples are collected during annual spring flow releases at 4 sampling locations on the Trinity River. From upstream to downstream, the locations are Trinity River at Lewiston (TRAL), Trinity River at Grass Valley Creek (TRGVC), Trinity River at Limekiln Gulch (TRLG), and Trinity River at Douglas City (TRDC). TRAL is about 3 river km downstream from Lewiston Dam, which severely limits the quantity of bed material supplied from upstream, whereas TRDC is more than 30 river km downstream from the dam and is downstream from several significant tributaries. For details on the sampling locations and sampling protocols, see Gaeuman et al. (2009).

Although bedload sampling has been performed annually at most of these locations since 2004, only the 2008 sample data were used for the analyses reported here. Approximately 30 bedload samples were collected on the rising limb of the 2008 release and about 20 samples were collected on the falling limb at each location. The 2008 data was selected because pre- and post-release bed surface pebble counts (necessary to quantify the bed states relevant to the rising and falling limbs of the hydrograph) are unavailable for earlier years. In addition, the 2008 flow release peaked at 170 m<sup>3</sup>/s, which is sufficient to entrain particles equal to or somewhat larger than  $D_m$ . By contrast, the 2007 and 2009 releases peaked at about 127 m<sup>3</sup>/s, such that the transported load consisted almost entirely of size fractions finer than  $D_m$ .

The bedload samples were used to estimate  $\tau_{rm}$  and  $\tau_{ri}$  for several size classes and for both limbs of the release via methods described by Wilcock and Crowe (2003) and Gaeuman et al. (2009). Estimates of  $\tau_{ri}$  were obtained for the following classes: 0.5-4 mm, 4-8 mm, 8-16 mm, 16-32 mm, and 32-64 mm. In addition, fractional bedload rating curves were developed for the same size fractions and for both limbs of the hydrograph by fitting the sample data to a shifted power function:

$$Q_b = a(Q - Q_c)^b \quad (2)$$

where  $Q_b$  is the bedload transport rate,  $Q$  is the water discharge,  $Q_c$  is the water discharge when sediment transport begins, and  $a$  and  $b$  are fitting parameters (Gaeuman et al. 2009).

The maximum discharge attained during the 2008 release is equivalent to about a 1.7-year event in the current regulated flow regime. Although this relatively modest flow was sufficient to produce transport of particles in the cobble size range, size classes larger than about 1.2 times  $D_m$  were transported only intermittently. As a result, the measured transport rates for these larger size fractions tend to be highly variable and frequently incorporate zero-mass samples even at the peak discharge. As rating curves and estimates of  $\tau_{ri}$  developed from such data are unreliable, a portion of the data pertaining to the 32-64 mm class and all of the 64-128 mm transport data were excluded from most of the results presented below.

## RESULTS

**Bedload Rating Curves** Bedload rating curves for most size classes were found to show a decrease in transport rates on the falling limb of the release, particularly for the finer fractions. This result is illustrated by Figure 1, in which fractional data are condensed into just 2 fractions (< 8 mm and > 8 mm) to conserve space.

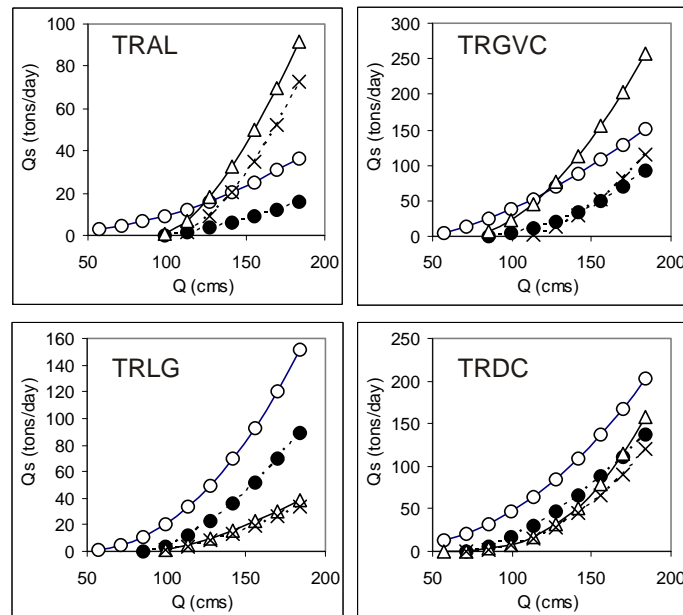


Figure 1 Bedload rating curves for fine and coarser size fractions at each sampling location. Open circles = rising limb, < 8 mm; filled circles = falling limb, < 8 mm; open triangles = rising limb, > 8 mm; X = falling limb, > 8 mm.

Decreases in transport rates between the rising and falling limbs can be seen to occur via 2 distinct modes: In many instances the falling-limb curve shows a substantial increase in the discharge necessary to initiate transport, i.e.,  $Q_c$  in equation 2 is larger on the falling limb. For example,  $Q_c$  for the < 8 mm transport curves at TRAL increase from near zero on the rising limb to 91  $m^3/s$  on the falling limb. Some other rating curve pairs for which the shift in  $Q_c$  is relatively modest have falling limb curves that are essentially scaled-down versions of the rising limb curves, as might be achieved by reducing the coefficient  $a$  in equation 2. Most pairs of curves show a combination of both modes of decrease, whereas a few pairs (> 8 mm at TRLG for example) show little if any evidence of bedload hysteresis.

Table 1 Selected bed surface and shear stresses parameters for the rising and falling limbs of the hydrograph for each sampling location.  $F_s$  refers to the fraction of “sand” on the bed surface, where “sand” is here defined as the 0.5-4 mm fraction.

	TRAL		TRGVC		TRLG		TRDC	
	Rise	Fall	Rise	Fall	Rise	Fall	Rise	Fall
$D_m$ (mm)	42	42	34	46	48	45	25	41
$\tau_{rm}$ (N/m <sup>2</sup> )	44.2	45.2	17.2	19.0	24.5	16.1	17.0	19.6
$\tau_{*rm}$	0.065	0.065	0.031	0.026	.031	.022	0.042	0.029
$\tau_r$ (16-32 mm class)	46.0	48.0	16.0	18.0	19.0	20.0	17.0	17.0
Change in $\tau_{r(16-32)}$	+4%		+12.5%		+5%		0%	
$\tau_r$ (0.5-4 mm class)	30.0	39.0	8.0	10.0	8.0	12.0	9.0	10.0
Change in $\tau_{r(0.5-4)}$	+30%		+25%		+50%		+11%	
$F_s$	0.04	0.04	0.08	0.05	0.04	0.05	0.10	0.04
$h$ (equation 1)	0.13	0.06	0.22	0.20	0.30	0.10	0.24	0.19

**Reference Shear Stresses** Comparisons of reference shear stresses obtained from rising versus falling limb sample data indicate that  $\tau_{ri}$  for the finest fractions tends to increase over the course of the hydrograph, whereas  $\tau_{ri}$  for larger particles remains essentially constant (Table 1). For example, the value of  $\tau_{ri}$  for the 0.5-4 mm fraction increased by an average of 29% across the 4 sampling locations, whereas the average increase for the 16-32 mm class is about 5%. Changes in  $\tau_{rm}$  over the hydrograph are slightly more difficult to interpret because the absolute magnitude of  $\tau_{rm}$  depends on the particle size referenced by  $D_m$ , which may also change over time. As shown in Table 1,  $D_m$  either remains relatively constant or increases, presumably because finer fractions are winnowed from the bed surface, such that changes in  $\tau_{rm}$  generally follow the changes in  $D_m$ . Values of  $\tau_{*rm}$ , on the other hand, consistently remain the same or decrease over time. Such a decrease is expected at locations where  $D_m$  increases, since larger particles are usually more exposed to the flow and so are associated with smaller dimensionless shear stresses. The simultaneous decrease in  $\tau_{*rm}$  and  $D_m$  at TRLG is mildly perplexing, but could be attributable to error in estimating one or the other parameter. With the possible exception of  $D_m$  at TRLG, all the changes in  $\tau_r$  observed for  $D_m$  and the 16-32 mm class indicate that the absolute shear stresses needed to entrain gravel particles of a given size at a particular location remained nearly constant over the flow release.

**Hiding-Exposure Relations** Ratios of  $\tau_{ri}/\tau_{rm}$  versus  $D_i/D_m$  for all size classes from both rising and falling limbs of the hydrograph and curves corresponding to several recently published hiding-exposure functions are plotted in Figure 2. Several of the relations evaluated here, i.e., those due to Duan and Scott (2008), Wu et al. (2000), and Wu and Yang (2004) fit the Trinity data poorly. The Wilcock and Crowe (2003) curve conforms to the plotted data much better, and the best fit is achieved by the Wilcock and Crowe relation as modified by Gaeuman et al. (2009). The success of this latter curve is not surprising, as it was developed using bedload transport data collected in the Trinity River in 2006 and 2007. It is interesting to note, however, that bedload transport rates computed with either the original Wilcock and Crowe equations or the calibrated equations presented by Gaeuman et al. (2009) greatly underestimate the actual bedload transport measured during the 2008 release. This failure is due to the fact that the maximum shear stresses attained during the 2008 release exceeded the values of  $\tau_{ri}$  for many size fractions only slightly or not at all. As noted by Barry et al. (2004), sensitivity to minor errors in estimates of  $\tau$  or of

mobility parameters is a significant weakness of equation that incorporate threshold-like entrainment parameters.

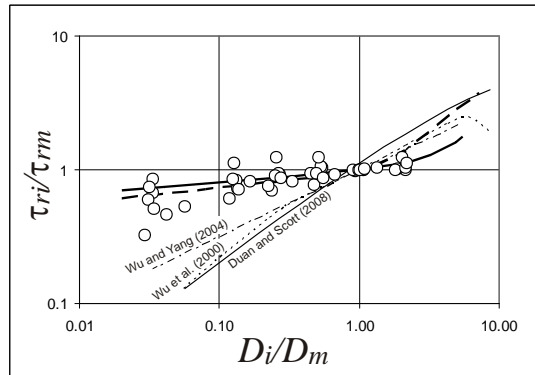


Figure 2 Reference shear stress ratios determined from bedload samples plotted as a function of grain size ratio for all size fractions, all sample locations, and both hydrograph limbs. Curves correspond to published hiding-exposure functions. Solid bold curve indicates the Gaeuman et al. (2009) calibration of the Wilcock and Crowe (2003) hiding function. Dashed bold curve is the original Wilcock and Crowe (2003) curve, and the other curves are as labeled.

Figure 3 shows values of  $\tau_{ri}/\tau_{rm}$  versus  $D_i/D_m$  segregated by sample location and hydrograph limb. At 2 of the 4 sampling locations (TRAL and TRLG) values of  $\tau_{ri}/\tau_{rm}$  for the finer particle fractions are substantially larger on the falling limb of the release than on the rising limb. Conversely,  $\tau_{ri}/\tau_{rm}$  tends to remain approximately constant, or even to decrease slightly, for particles with  $D_i/D_m$  near 1. Thus, the difference between the rising and falling data at TRAL and TRLG has the appearance of a clockwise rotation of the trend lines around a pivot located at a point with a value of  $D_i/D_m$  of about 1 or 2, such that the slope of the trend line, which is equivalent to  $h$  in equation 1, decreases on the falling limb. Differences between the rising- and falling-limb data at the remaining 2 sampling locations (TRGVC and TRDC) are too small to be considered a real change, but it is fair to say that neither site indicates an increase in the slope of the trend lines.

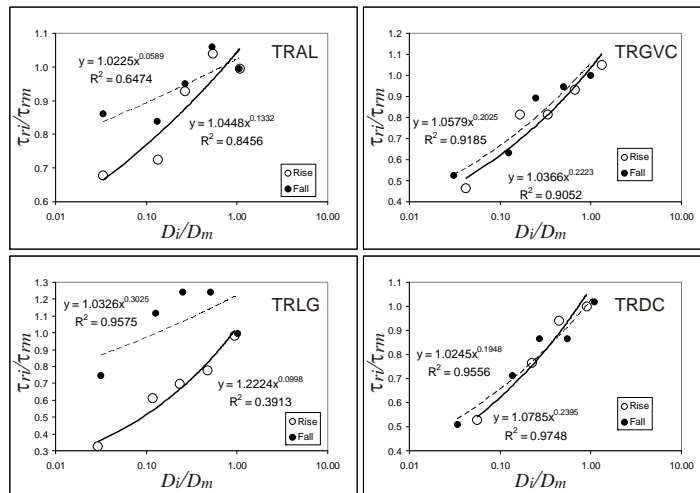


Figure 3 Reference shear stress ratios versus  $D_i/D_m$  by sample location and hydrograph limb. Note that the abscissa is arithmetic.

## DISCUSSION

**Hysteresis Due to Change in the Bed Surface Distribution** A portion of the bedload hysteresis evident in the 2008 Trinity River can be described in terms of a scaling of the coefficient  $a$  in the bedload rating relations. It is likely that at least a portion of this scaling is due to changes in the relative abundance of particles in the different size classes. For example, if particle of a size class  $i$  are winnowed from the stream bed during the flow release,  $F_i$  will decrease and fewer particles in class  $i$  will be available for transport on the falling limb. The fractional transport rate of class  $i$  should therefore decline even if the absolute mobility of the class remains constant. Assuming that  $F$  decreases for the more mobile particle classes, which is compensated for by an increase in the relative abundance of less mobile classes, the net effect should be a decrease in the total transport rate. In simplest terms, these changes essentially boil down to a general coarsening of the bed.

To test the validity of this explanation, each limb of the rating curves for several size fractions at TRDC were scaled by rising- and falling-limb values of  $F_i$ . This particular set of data were selected for this analysis because the shift in  $Q_c$  between the rising- and falling-limb rating curves is minor, such that the hysteresis appears to be mainly due to scaling of the curves. As shown in Figure 4, correcting these rating curves for changes in  $F_i$  largely removes any evidence of bedload hysteresis. It appears that changes in  $F_i$  may explain some instances of hysteresis, but this straight-forward mechanism cannot account for instances of hysteresis where  $F_i$  does not decrease or where  $Q_c$  is shifted.

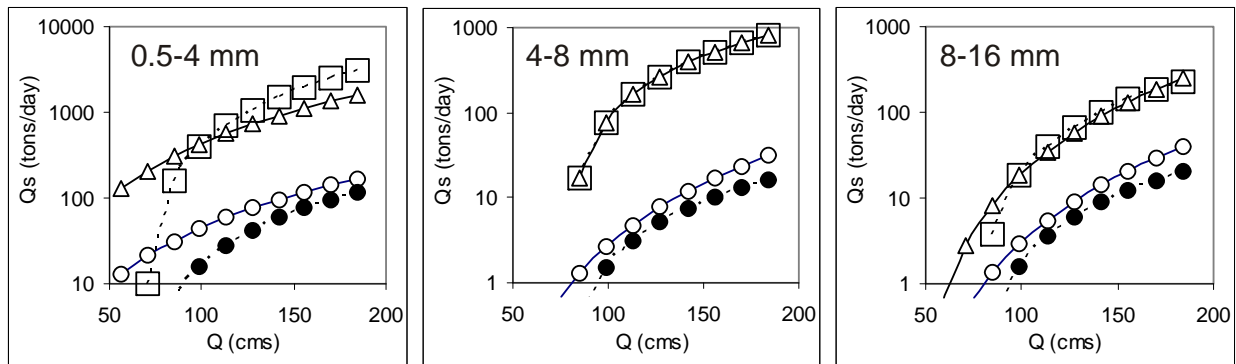


Figure 4 Fractional bedload rating curves and normalized fractional bedload rating curves for selected size fractions at TRDC. Open circles = rising limb; filled circles = falling limb; open triangles = rising limb normalized for  $F_i$ ; open squares = falling limb normalized for  $F_i$ . Note that the 0.5-4 mm curves incorporate a relatively strong shift in  $Q_c$  compared to the other fractions shown.

**Hysteresis Due to Changes in Reference Shear Stresses Constant  $\tau_{rm}$**  It is well documented that gravel entrainment is facilitated by the presence of sand on the stream bed (Jackson and Beschta 1984; Wilcock et al. 2001; Curran and Wilcock 2005). As sand is winnowed and  $F_s$  decreases over the course of a hydrograph, as indeed it did at 2 of the 4 sampling locations, values of  $\tau_r$  for all size fractions should generally increase. However, this is not the case for the 2008 Trinity River data, which indicate that  $\tau_r$  remained essentially constant for particles within about 2 phi classes of  $D_m$  irrespective of any changes in the bed surface particle size distribution that occurred during the flow release. Moreover, the mobility of these particles is apparently

independent of changes in the mobility of the sand and fine gravel fractions, for which  $\tau_r$  was found to increase substantially over time.

The lack of a clear relationship between  $\tau_{rm}$  and  $F_s$  is in need of explanation. One possibility is that values of  $F_s$  determined prior to and following the flow release do not represent the quantity of sand present on the bed at the higher discharges when gravel transport occurs. It is plausible that the effective  $F_s$  that covers the bed during active periods of bedload transport is maintained at a high level by a large sand flux from sediment reservoirs located far upstream, including sand-filled pools, banks, and sandy bar deposits. Similarly, the  $F_s$  observed at baseflow discharges may represent little more than the residue left behind after the incoming flux has waned and most of the sand in the immediate vicinity of the sampling transect has been swept downstream by the tail of the hydrograph. This hypothesis is particularly attractive because it also seems to explain the fact that values of  $\tau_{ri}$  are generally 2 or 3 times larger at TRAL than at the other 3 locations (Table 1). A single relatively minor tributary enters the Trinity River between TRAL and Lewiston Dam, so the natural sediment supply to the site is very small and significant reservoirs of sand in the reaches upstream are lacking. Thus, the effective  $F_s$  during the release is unlikely to be substantially greater than its baseflow value of 0.04.

**Hiding-Exposure Relations** It has been shown above that  $\tau_{ri}$  increased over the course of the 2008 release hydrograph for particle size fractions smaller than medium gravel, but that  $\tau_{ri}$  for particle sizes approaching  $D_m$  remained roughly constant. Together, these changes are manifested as a decrease in the slope of the relation between  $\tau_{ri}/\tau_{rm}$  and  $D_i/D_m$  over the range of all  $D_i/D_m$  less than about 1 or 2. This change in slope is equivalent to a decrease in the exponent  $h$  in equation 1, and indicates that the bedload transport process more closely approximated equal mobility on the falling limb of the 2008 release than on the rising limb. On average,  $h$  decreased by a factor of about 1.6 between the two hydrograph limbs, from an average of about 0.22 on the rise to about 0.14 on the fall (Table 1). All values of  $h$  fall within the range of 0-0.3 reported by other investigators.

The slope changes shown on Figure 3 have the appearance of a clockwise rotation about a pivot that appears to be located at a value of  $D_i/D_m$  near 1 or somewhat larger than 1 for some sample locations. However, sparse bedload transport in the larger size classes precludes drawing firm conclusions regarding the form of the hiding-exposure relation for particles larger than  $D_m$ . Nonetheless, it can be surmised from fractional bedload rating curves that the hiding-exposure relations for coarse particle sizes change relatively little between the rising and falling hydrograph limbs. Fractional rating curves for the finer particle size fractions typically show larger changes in  $Q_c$  between hydrograph limbs, and greater hysteresis in general, than is observed in the curves for the coarser fractions (Figure 1).

A critical point to be drawn from these results is that particle hiding effects may be far more dynamic than is implied by many bedload transport functions, which often employ a single hiding-exposure curve that is apparently expected to be widely applicable. A second key point is that hiding-exposure relations appear to consist of at least two and perhaps three segments, each of which displays distinct dynamics. It appears that the complete curve consists of a fine tail (particles finer than about 0.4 times  $D_m$ ) over which  $\tau_{ri} < \tau_{rm}$  and the slope of the curve varies rapidly in response to recent flow history and changes in  $F_i$  for the finer size fractions. The

hiding-exposure curve also contains of a central segment (particles between about 0.4 and 1.2 times  $D_m$ ) over which  $\tau_{ri} \sim \tau_{rm}$  and particle entrainment can be accurately characterized in terms of near perfect equal mobility. In their analysis of Trinity River bedload samples collected in 2006, Gaeuman et al. (2009) concluded that the slope of the hiding-exposure relationship was small for particles finer than about 3 times  $D_m$ . It is therefore hypothesized that the range of approximate equal mobility spans 2 or perhaps 3 phi classes in total. The actual shear stress necessary to mobilize particles within this range of the size distribution remains essentially constant over the short and medium time scales, irrespective of short-term changes in the smaller size fractions. However,  $\tau_r$  for these size fractions can differ markedly from one location to another, and can undoubtedly also change slowly at individual locations over relatively long time periods. Finally, the complete hiding-exposure curve includes a segment corresponding to particles coarser than about 2 times  $D_m$  for which  $\tau_{ri} > \tau_{rm}$ . Although the 2008 bedload data presented herein yields no information about the characteristics of that portion of the curve, previous investigations (Parker and Klingeman 1982; Wilcock and Crowe 2003; Gaeuman et al. 2009) indicate that the slope of the hiding-exposure relation increases over this range of particle sizes. Whether the slope of the curve through the coarse tail of the particle size distribution is static or whether it changes dynamically in a manner similar to the fine tail is an open question.

## CONCLUSION

The data and analyses presented here suggest that bedload hysteresis observed during the 2008 flow release in the Trinity River is be at least partially accounted for by changes in the hiding-exposure relation between different particle size fractions, i.e., equation 1. The available information points to a clockwise rotation in the hiding-exposure relation that corresponds to greater equal mobility among particles sizes on the falling limb. However, the shift toward greater equal mobility on the falling limb was achieved exclusively by a decrease in the mobility of the finest grains. The shear stresses needed to mobilize particles in the central portion of the particle size distribution remained nearly constant over the course of the release hydrograph at individual sampling locations, even though spatial variability between the sampling locations was observed. These finding indicate that the mobility of different grain sizes adjust to changes in flow and sediment supply on different time scales. For the finer particle fractions in the size distribution,  $\tau_{ri}$  can change significantly over a single flow event, whereas the mobility of coarser particles varies little over similar time periods. In addition,  $\tau_{ri}$  was found to be nearly constant over the size range spanning about 0.4 times  $D_m$  to at least 1.2 time  $D_m$ . Although little reliable information for evaluating the relative mobility of particles larger than 1.2 times  $D_m$  is available in these data, previously published analyses suggest that the range of approximate equal mobility may extends to particle sizes as large as 2 times  $D_m$  or more.

## REFERENCES

- Andrews, E.D., (1994), "Marginal bed load transport in a gravel bed stream, Sagehen Creek, California," *Water Resources Research*, 30, 2241-2250.
- Ashworth, P.J., and R.I. Ferguson, (1989), "Size-selective entrainment of bed load in gravel bed streams," *Water Resources Research*, 25, 627-634.
- Ashmore, P.E. and M.A. Church, (1998), "Sediment transport and river morphology: A paradigm for study," In *Gravel-bed Rivers in the Environment*, P.C. Klingeman, R.L.

- Beschta, P.D. Komar and J.B. Bradley, eds. Water Resources Publications, LLC. Highlands Ranch, CO, pp 115-148.
- Barry, J.J., J.M. Buffington, and J.G. King, (2004), "A general power equation for predicting bed load transport in gravel bed rivers," *Water Resources Research*, 40, W10401, doi:10.1029/2004WR003190.
- Curran, J.C. and P.R. Wilcock, (2005), "Effect of sand supply on transport rates in a gravel-bed channel," *Journal of Hydraulic Engineering*, 131(11):961-967.
- Duan, J.G. and S. Scott, (2008), "Selective bed-load transport in Las Vegas Wash, a gravel-bed stream," *Journal of Hydrology*, 342, 320-330.
- Ferguson, R.I., K.L. Prestegard, and P.J. Ashworth, (1989), "Influence of sand on hydraulic and gravel transport in a braided gravel bed river," *Water Resources Research*, 25, 635-643.
- Gaeuman, D., E.D. Andrews, A. Krause and W. Smith, (2009), "Predicting fractional bedload transport rates: application of the Wilcock-Crowe equations to a regulated gravel-bed river", *Water Resources Research*, 45, W06409, doi:10.1029/2008WR007320.
- Gomez, B., and M. Church, (1989), "An assessment of bed load sediment transport formulae for gravel bed rivers," *Water Resources Research*, 25, 1161-1186.
- Jackson, W. L., and R. L. Beschta, (1984), "Influences of increased sand delivery on the morphology of sand and gravel channels," *Water Resources Bulletin*, 20(4), 527-533.
- Martin, Y., (2003), "Evaluation of bed load transport formulae using field evidence from the Vedder River, British Columbia," *Geomorphology*, 53(1):75-95.
- McLean, D.G., M. Church, and B. Tassone, (1999), "Sediment transport along the lower Fraser River: 1. Measurement and hydraulic computations," *Water Resources Research*, 35(8):2533-2548.
- Parker, G., (1990), "Surface-based bedload transport relation for gravel rivers," *Journal of Hydraulic Research*, 28:417-436.
- Parker, G., and P.C. Klingeman, (1982), "On why gravel bed streams are paved," *Water Resources Research*, 18, 1409-1423.
- Wilcock, P.R. and J.C. Crowe, (2003), "Surface-based transport model for mixed-size sediment," *Journal of Hydraulic Engineering*, 129:120-128.
- Wilcock, P.R., S.T. Kenworthy and J.C. Crowe, (2001), "Experimental study of the transport of mixed sand and gravel.," *Water Resources Research*, 37(12):3349-3358.
- Wu, W., S.S.Y. Wang, and Y. Jia, (2000), "Nonuniform sediment transport in alluvial rivers," *Journal of Hydraulic Research*, 38(6):427-434.
- Wu, F.-C. and K.-H. Yang, (2004), "A stochastic partial transport model for mixed-size sediment: Application to assessment of fractional transport," *Water Resources Research*, 40, W04501, doi:10.1029/2003WR002256.